Numerical experiments in high frequency diffraction theory

Pat F. Daley

ABSTRACT

Formulae for diffraction theory in elastodynamic media, based on the high frequency Asymptotic Ray Theory (ART) formulation are presented. The original papers and texts from which the formulae used here were obtained are highly mathematical, and the progression from theory to the development of associated software is not a straightforward endeavour. This paper addresses the diffraction of seismic waves by linear edges, employing an extension of zero order asymptotic ray theory. This extension is obtained through the implementation of the boundary layer method. To provide some initial insight into this problem for the elastodynamic case, a few simple models were chosen for analysis. The motivation for this was to establish a basis for the extension of diffraction theory to more complicated and realistic geological structures. Program packages, based on ART, dealing with these structure types are common in seismic modeling software packages. However, at present their use is limited, with a few exceptions, to modeling of only reflected seismic response recorded at the earth's surface, or vertical seismic profile (VSP) arrays as a result of some form of point source media excitation. The inclusion of diffracted arrivals in these packages would produce more realistic synthetic traces, enhancing their usefulness.

Also discussed is how complicated seismic diffracting structures may be divided into a configuration consisting of several linear edge components so that the total diffracted response from the more complicated structure is the sum of these individual linear edge building blocks.

INTRODUCTION

The works of Klem-Musatov (1986 (1995)) and Klem-Musatov et al. (2008) deal with elastic waves diffracted by the linear edges of seismic interfaces. An extension of Asymptotic Ray Theory (ART), was employed to obtain a high frequency approximation to waves diffracted by linear edges. Discussions of ART may be found in the works of Hron and Kanasewich (1971), Červený and Ravindra (1971) where the work of Gel'chinsky (1961) is summarized, Červený and Hron (1980) which contains the theory of Dynamic Ray Tracing (DRT), and Červený (2001), among others. The diffraction theory employed here employs modifications of ART and DRT, which requires introducing the boundary layer method and utilizing analytic continuation for explaining some of the more subtle points. The theory is valid for the three dimensional case of rays emanating from a point source. The text by Klem-Musatov (1980), once relatively inaccessible as it was written in Russian now appears in an English translation, Klem-Musatov (1995). A work based on the original Russian text may be found in the PhD. thesis of Chan (1986), where many of the topics contained in that text are addressed. Subsequent papers by Bakker (1990), Hron and Chan (1995) and Gallop and Hron (1997) contain selected analysis of this theory. What follows from these papers is that any final formulae for a diffracted wavefield would ideally be such that they: (a) would allow for simple physical interpretation, (b) provide a practical means for the efficient calculation

of the diffracted field and (c) maintain a reasonable degree of accuracy when describing the diffracted wavefield.

The above conditions require an accurate approximation of the diffracted wavefield, based on sound physical and mathematical principles, which can be incorporated into existing programs for the computation of synthetic seismograms for complex geological models. This approximation would preferentially employ a zero order ART solution for the incident wave field at the diffracting edge multiplied by a diffraction coefficient. The resulting diffracted field is obtained by considering the diffracting edge as a source of seismic energy and tracing its minimum time path to receivers and include the effects of any interactions with seismic boundaries as well as geometrical spreading in its amplitude. The theory may be referred to as 2.5 D as out of plane geometrical spreading is included.

The accuracy of a method similar in development to the one described above was presented in the work of Chan (1986) where a geometrical optics (high frequency) method for the reflected and diffracted contributions to the SH wavefield was compared with the highly numerically accurate results obtained by the Alekseev-Mikhailenko Method (AMM). The AMM is a hybrid technique for constructing the total elastodynamic wavefield response of a complex three dimensional geological model due to point source excitation, assuming, in this application, an uncommon usage of radial symmetry. A combination of finite integral tranforms and finite difference methods was employed to achieve this (Mikhailenko, 1985).

As the treatment of this problem contained in Klem-Musatov (1995) and Chan (1986) is quite comprehensive, only minimal theoretical developments of the problem will be presented here. For clarity, the problem will be defined in the next section along with some comments and a restatement of the final formulae required for computation of the wavefield due to an edge diffractor will be presented. Other sources of intermediate theoretical and numerical development (Hron, 1986 and Daley, 1990) might be of some use for those interested in the theoretical development of this problem. However, these reports are fairly mathematically intense and of minimal attraction to the majority of readers.

THEORETICAL OVERVIEW

Consider a three dimensional Cartesian coordinate system (r, y, z), in a halfspace $z > 0$ with an explosive point source of compressional (P) waves located at the origin, (Figures (1) and (2)). A semi-infinite wedge is assumed to be located at a depth $z_{\mathcal{D}}$ below the surface, occupying the three dimensional space ($z_{\mathcal{D}} \le z < \infty$, $0 \le r \le r_{\mathcal{D}}$, $-\infty < y < \infty$). Receivers are placed both at the surface and in a vertical array (VSP) in the (r, z) plane containing the source. For the VSP case only the direct and diffracted P arrivals will be included in the synthetic traces while for the surface receivers (AVO) the reflected compressional (P) wave from the top horizontal boundary of the wedge and the diffracted *P* wave from the edge at $\mathcal{D} = (r_{\mathcal{D}}, z_{\mathcal{D}})$ are the

only arrivals considered The compressional (P) wave velocities in the half plane, α, and in the wedge strip, α_1, are chosen such that $\alpha < \alpha_1$. The shear wave (S_V) velocities are defined by the relation $\beta = \alpha/\sqrt{3}$ and the densities are obtained from Gardner's Law. This will be referred to as Model I. In a later section a modification of Model I will be considered, denoted as Model II and shown schematically in Figure 3.

When considering diffraction from the wedge in Model I there are two regions to be considered in the half plane, the illuminated (Ω_I) and the shadow (Ω_S) regions (Figures (1) and (2)). These regions are different for the AVO and VSP situations. The shadow region consists of all points that do not lie in the "direct line of sight path" from the source. (This assumes that possible energy propagation through the elastic wedge strip is not considered.) The illuminated and shadow regions are separated from one another by what is termed the "boundary ray". In the simple situations being considered here the direct and reflected arrivals only appear on the synthetic traces in the illuminated regions while the diffracted arrival exist in both regions. As an example, for the AVO case from $r_M = 0$ to $r_M = 2r_{\mathcal{D}}$ at $z = 0$, both the reflected and diffracted *P* waves may be registered at a surface receiver. Beyond $r_M = 2r_{\mathcal{D}}$ only the diffracted *P* arrival is recorded.

The Fourier time transformed vector particle displacement of an incident compressional wave generated at the point source at the origin 0 and recorded at the vertical or surface receiver arrays may be written in terms of the zero order ART approximation as

$$\mathbf{U}_G(\mathbf{r},\omega) = \frac{F(\omega)\mathbf{\Pi}}{L_G(\mathbf{r})}\exp\left[i\omega\tau_G(\mathbf{r})\right]\mathbf{e} \tag{1}$$

where the subscript "G" (geometrical) indicates either the direct or reflected P arrival, $\mathbf{r}$ is the generally three dimensional position vector of some point in the halfspace that may, when convenient be denoted as M, ω is the circular frequency, $\tau_G(\mathbf{r})$ $\left[\tau_G(M)\right]$ is the travel time along the ray from the source to some point $\mathbf{r}$, $L_G(\mathbf{r})$ $\left[L_G(M)\right]$is the 3D geometric spreading of the ray between the source and the point $\mathbf{r}$ which for the direct arrival case is given by

$$\frac{1}{L_G(\mathbf{r})} = \frac{1}{R_M} = \frac{\cos\theta_0}{z_M} \quad (z_M \le z_{\mathcal{D}}). \tag{2}$$

and for the reflected arrival as

$$\frac{1}{L_G(\mathbf{r})} = \frac{1}{R_M} = \frac{\sin\theta_0}{r_M} \quad (0 \le r_M \le r_{\mathcal{D}}). \tag{3}$$

In terms of the ray parameter p, the direct and reflected arrival times may be written as

(Aki and Richards, 1980)

$$\tau_G(p) = r_M p + z_M\left(\alpha^{-2} - p^2\right)^{1/2} \quad \text{(Direct)}. \tag{4}$$

$$\tau_G(p) = r_M p + 2z_{\mathcal{D}}\left(\alpha^{-2} - p^2\right)^{1/2} \quad \text{(Reflected)}. \tag{5}$$

Minimizing $\tau_G(p)$ produces the values of p that gives the minimal travel times, i.e.,

$$\frac{d\tau_G(p)}{dp} = r_M - \frac{z_M p}{\left(\alpha^{-2} - p^2\right)^{1/2}} = 0 \quad \text{at } p = p_0 \quad \text{(Direct)}. \tag{6}$$

$$\frac{d\tau_G(p)}{dp} = r_M - \frac{2z_{\mathcal{D}} p}{\left(\alpha^{-2} - p^2\right)^{1/2}} = 0 \quad \text{at } p = p_0 \quad \text{(Reflected)}. \tag{7}$$

so that

$$p_0 = \frac{r}{\alpha\left[z_M^2 + r_M^2\right]^{1/2}} = \frac{\sin\theta_0}{\alpha} \quad \text{(Direct)}. \tag{8}$$

and

$$p_0 = \frac{r_M}{\alpha\left[\left(2z_{\mathcal{D}}\right)^2 + r_M^2\right]^{1/2}} = \frac{\sin\theta_0}{\alpha} \quad \text{(Reflected)}. \tag{9}$$

The term $\mathbf{\Pi}$ in equation (1) is the product of all reflection and transmission coefficients encountered along the geometrical ray from source to receiver. In the VSP case, $\mathbf{\Pi} = 1$ and in the AVO case $\mathbf{\Pi} = PP(p_0)$, the reflection coefficient at the halfspace/wedge boundary. The vector $\mathbf{e}$ is either the vector decomposition of the incident particle displacement at a receiver into vertical and horizontal components or the surface conversion coefficient vector $\mathbf{P}_C(p_0)$ which partitions the particle displacement at the receiver into vertical and horizontal components at a surface receiver and is defined as

$$\mathbf{P}_C(p_0) = \left[P_{CV}, P_{CH}\right]^T. \tag{10}$$

The superscript "T" indicates *transpose*, and "H" and "V" refer to horizontal and vertical components of the vector $\mathbf{P}_C(p_0)$. Expressions for the reflection and surface conversion coefficients may be found in Červený and Ravindra (1971). $F(\omega)$ is the Fourier time transform of the band limited source wavelet, $f(t)$, t being time. A spherically symmetric radiation pattern of this source function is assumed.

For the diffracted arrival the travel time from source to receiver consists of two parts; the time it takes the ray to travel form the source to the diffraction edge in the (r,z) plane at $(r_{\mathcal{D}}, z_{\mathcal{D}})$ plus the time taken for the ray to progress from the diffraction point to the receiver. This infers that a diffracted arrival generally has a different ray parameter on either side of the diffraction point. This will be dealt with shortly.

From the works of (Klem-Musatov, 1995 and Klem-Musatov et al., 2007) to the elastodynamic case, the diffracted particle displacement at some point **r** recorded at some receiver due to the diffraction edge in the (r,z) plane at $\mathcal{D}=(r_{\mathcal{D}},z_{\mathcal{D}})$ may be written as

$$\mathbf{U}_{\mathcal{D}}(\mathbf{r},\omega)=\frac{F(\omega)I(\omega,\psi)\mathbf{\Pi}}{L_{\mathcal{D}}(\mathbf{r})}\ \exp\left[i\omega\tau_{\mathcal{D}}(\mathbf{r})\right]\mathbf{e}. \tag{11}$$

Apart from the introduction of the subscript "$\mathcal{D}$", which refers to diffraction, the only difference between equations (1) and (11) is the term $I(\omega,\psi)$, which is the radiation characteristic of the diffracted wave at a unit distance from the diffraction edge at $\mathcal{D}$. The angle ψ is the angle measured from the shadow/illuminated region boundary and chosen as negative in the illuminated region and positive in the shadow region. (See Figures (1) and (2)). The geometrical spreading $L_{\mathcal{D}}(\mathbf{r})=L_{\mathcal{D}}(M)$ is the three dimensional geometrical spreading from the source to the point of diffraction plus the addition of the geometrical spreading from this point, assumed to be a point source, to M, so that

$$\frac{1}{L_{\mathcal{D}}(M)}=\frac{1}{R_{0\mathcal{D}}+R_{\mathcal{D}M}}\qquad\frac{1}{R_{0\mathcal{D}}}=\frac{\cos\theta_0}{r_{\mathcal{D}}}\qquad\frac{1}{R_{\mathcal{D}M}}=\frac{\cos\theta_{\mathcal{D}}}{(r_M-r_{\mathcal{D}})}. \tag{12}$$

and the diffracted travel time $\tau_{\mathcal{D}}(M)$ is

$$\tau_{\mathcal{D}}(M)=\frac{\left[h^2+r_{\mathcal{D}}^2\right]^{1/2}}{\alpha}+\frac{\left[z_{\mathcal{D}}^2+(r_M-r_{\mathcal{D}})^2\right]^{1/2}}{\alpha} \tag{15}$$

for both the VSP and AVO cases. The parameter $\theta_{\mathcal{D}}$ is the acute angle the incidence the ray at the receiver makes with the vertical and is equal to $\tan^{-1}(r_{\mathcal{D}}/z_{\mathcal{D}})$.

It is convenient at this point to introduce another Cartesian coordinate system, (u,v), whose origin is at $\mathcal{D}$, together with a related polar coordinate system, (ρ,ψ). As before, ψ is positive/negative in the shadow/illuminated regions which are defined by the boundary ray. The quantity ρ_M is the distance from the point of diffraction at $\mathcal{D}$ to some observation point M fully defined by the additional coordinate, $\psi_{\mathcal{D}}$ within the context of the Cartesian system (u,v).

The radiation characteristic function $I(\omega,\psi)$, which is measured a unit distance from $\mathcal{D}$ will be replaced in Equation (11) by the more general related function, $\mathrm{W}(\omega,w(\omega,\rho,\psi))$, termed the diffraction coefficient. The vector particle displacement at the point $M=(\rho_M,\psi_M)$, which is contained in either the surface or vertical receiver arrays at the coordinates (ρ_M,ψ_M) may be written as

$$\mathbf{U}_{\mathcal{D}}\ (M,\omega)=\frac{W(\omega,w_M)\,\mathbf{\Pi}}{L_{\mathcal{D}}(M)}\ \exp\left[-i\omega\left(t-\tau_{\mathcal{D}}(M)\right)\right]\mathbf{e}\,. \tag{16}$$

where $w_M \equiv w(\omega,\rho_M,\psi_M)$, with ω being the circular frequency. The geometrical spreading $L_{\mathcal{D}}(M)$ and arrival time $\tau_{\mathcal{D}}(M)$ for the diffracted *P* arrival for both cases of model I are

$$L_{\mathcal{D}}(M)=\left[z_{\mathcal{D}}^2+r_{\mathcal{D}}^2\right]^{1/2}+\rho_M\,. \tag{17}$$

$$\tau_{\mathcal{D}}(M)=\frac{\left[z_{\mathcal{D}}^2+r_{\mathcal{D}}^2\right]^{1/2}}{\alpha}+\frac{\rho_M}{\alpha} \tag{18}$$

respectively. To reiterate, the compressional wave velocity in the halfspace, except for the wedge is α. All other quantities have been previously defined.

To evaluate the diffraction coefficient both the diffracted travel time, $\tau_{\mathcal{D}}(M)$, and the direct or reflected P travel time, $\tau_G(M)$, are required. Referring to Figures (1) and (2), $\tau_G(M)$, has either the form

$$\tau_G(M)=\frac{\left[z_M^2+r_M^2\right]^{1/2}}{\alpha}\quad(\text{Direct}) \tag{19}$$

or

$$\tau_G(M)=\frac{\left[\left(2z_{\mathcal{D}}\right)^2+r_M^2\right]^{1/2}}{\alpha}\quad(\text{Reflected}) \tag{20}$$

The diffraction coefficient in Equation (16) $W(\omega,w)$ is now considered, omitting its derivation, as it is beyond the scope of this paper. Interested readers are referred to any of the earlier cited works where this aspect of the problem is fully addressed. This function is defined as

$$W(\omega,w)=\pm\frac{\exp\left[-i\pi w^2/2\right]}{2\sqrt{\pi}}\ \Gamma\left(1/2,-i\pi w^2/2\right) \tag{21}$$

where $\Gamma\left(1/2,-i\pi w^2/2\right)$ is the incomplete gamma function and for the illuminated zone

$$w^2=\left[\frac{2\omega}{\pi}\left(\tau_{\mathcal{D}}(M)-\tau_G(M)\right)\right] \tag{22}$$

while for the shadow zone

$$w^2 = \left[\frac{2\omega}{\pi} \left(\frac{\rho_M}{\alpha} (1 - \cos\psi_M) \right) \right] \tag{23}$$

Equation (22) for w^2 results from the fact that at some points on the surface no reflected arrival exists. This formula was obtained using analytic continuation and Appendix A contains a discussion of its derivation which is somewhat less than mathematically rigorous.

The operative phrase describing the transition from illuminated to the shadow region is "smoothly varying". This is achieved by employing analytic continuation of the ART solution across the boundary layer (boundary ray) separating these two zones. Any part of the solution, either kinematic or dynamic, that does not have this property should be considered as suspect.

The incomplete gamma function, $\Gamma(1/2, s)$ is defined as

$$\Gamma(1/2, s) = \int_s^\infty \frac{e^{-u}}{\sqrt{u}}\, du \ . \tag{24}$$

and may be written in terms of Fresnel integrals ($Ci(s)$ and $Si(s)$) or the complementary error function ($erfc(s)$), (Abramowitz and Stegun (1980)). However, due to the existence of tested software, specifically the subroutine *WOFZ* (Gautschi (1980), (1969)), and defined as

$$W(z) = e^{-z^2} erfc(-iz)\ , \tag{25}$$

for complex z, it was determined, after comparison with other algorithms, to employ this routine in numerical computations due to its accuracy (14 to 16 floating point digits if double precision accuracy is used). Thus Equation (20) may be rewritten so that the diffraction coefficient has the new form

$$W(\omega, w) = \pm W(z), \quad z = e^{i\pi/4} \sqrt{\omega/2}\, w \tag{26}$$

where the dependence of $W(z)$ on frequency is implied. Here, it may be useful to write down the asymptotic expansions for $erfc(z)$ and $W(z)$ for large values of $|z|$, $|\arg(z)| < 3\pi/4$.

$$erfc(z) \approx i\, e^{z^2} / \sqrt{\pi}\, z \tag{27}$$

$$W(z) \approx i/\sqrt{\pi} \left(e^{i\pi/4} \sqrt{\pi/2}\, w \right) = e^{i\pi/4} / \sqrt{\pi\omega(\tau_D - \tau_R)} \tag{28}$$

indicating that the amplitude of the diffracted arrival is of the order $O\left(1/\sqrt{\omega}\right)$ for large values of the argument of z.

Another simple geological model, depicted schematically in Figure (2) and denoted as Model II, will now be examined. It is similar to Model I with the exception that the wedge now occupies the space $(r_{\mathcal{D}} \le r < \infty, z_{\mathcal{D}} \le z < \infty, -\infty < y < \infty)$ in the halfplane $(z > 0)$. The expressions for the reflected and diffracted waves amplitudes and travel times are given by Equations (1) and (11), and (18) and (20) still hold, provided the coordinate system (ρ, ψ) is properly defined. The VSP problem will not be considered for this model as both the direct and diffracted arrivals have geometrical paths for energy propagation from source to receivers. The compressional wave velocities in this case are chosen such that $\alpha > \alpha_2$ and all of the velocities and volume densities describing the model are given in Table II. The major difference in the arrivals at the surface for this model is that the reflected arrival appears only at offsets *greater* than $(r = r_M = 2r_{\mathcal{D}})$. As is the previous model, the diffracted P event may be seen at all offsets.

Models I and II may now be combined to produce Model III (Figure (4)). This model is marginally more complicated than either of the two previous cases, but the reflected and diffracted wavefields are additive so that the seismic response of Model III is just the sum of the wavefields of Models I and II. In this manner, obtaining the diffracted wavefield for more complicated geological models may be reduced to computing the diffracted contributions due to individual edge diffractors and additively obtaining the total response as the cumulative sum of these elementary building blocks. There is no reason, however, for not including converted phase. It may be inferred that this process may be extended to truly three dimensional geological models by utilizing edge diffractors as the elementary structural quantity.

There are some additional points that should be given some consideration regarding the method of introducing diffracted amplitudes into the computation of synthetic traces using the method described here.

(1). Only "primary" diffractions are computed. That is, a given point diffractor may in practice excite another point diffractor. As the expressions given are high frequency approximations, the amplitude of the primary diffraction decays as $\omega^{-1/2}$ (Equation (28), so that the amplitude of the secondary diffraction would decay as ω^{-1}. For this reason it is not considered.

(2). It is possible, given the proper circumstances, for a critically refracted (head) wave to excite a point diffractor. Again, as the formulae presented here are high frequency approximations, this combination would decay as $\omega^{-3/2}$ (Červený and Ravindra, (1971)). The reason given above would also preclude the inclusion of this type of arrival in the present level of program development.

(3). To keep matters as simple as possible only PP direct, reflected and diffracted arrivals were presented in this report. *(PS)/(SP)* reflections and diffractions are similar in form as PP the in the high frequency limit. These diffractions decay as $\omega^{-1/2}$, the same as in the PP case. The same is also true for multiple reflections.

(4). Finally, the problem of possible diffraction within the wedge(s) should be mentioned. The refracted PP or PS wave at the point D will produce this effect. It has not been treated here in order to keep the discussion as simple as possible. However, in future applications to complex geological models, this facet of the theory will have to be investigated.

NUMERICAL RESULTS

The geological parameters defining the models mentioned earlier in this report are given in Tables I and II. Additional quantities required for model definition are the distance from the surface to the tops of the wedges, $h = 400m$, the horizontal distance from the source location to the points of diffraction, $r_D = 1000m$ and the horizontal distance from the source to the points the boundary ray in Models I and II with surface receiver arrays are both $r_B = 2000m$. The offsets of all of the synthetic seismograms presented run from $0m$ to $3000m$ in steps of $50m$. The VSP receiver line is at an offset of $1500m$ with receivers set at $25m$ intervals at depths of $100m$ to $1600m$. These together with a time scale and a brief description of what is shown in a given figure appear on all of the synthetic seismograms. A Gabor wavelet is used when producing the synthetic traces.

Schematics of the models used are given in Figures (1), (2), (3) and (4) where additional information may be found. The synthetic seismograms presented include both the vertical and horizontal components of displacement either at the surface or in a vertical array for an elastic halfspace with an embedded wedge or wedges.

Figures (8) through (11) are associated with Model I with Figures (8) and (9) displaying the vertical and horizontal components of displacement of the direct and diffracted arrivals. The vertical and horizontal components of the surface recorded reflected PP and diffracted arrivals are shown in Figures (10) and (11). There are 3 panels in each of the Figures (8) – (11)), showing: (a). the direct or reflected arrival, (b). the diffracted arrival and (c). the combination of the two. The PP reflection coefficient related to the halfspace/Wedge I interface may be seen in Figure (6.a). The vertical and horizontal components of the surface conversion coefficients are given in Figures (7.a) and (7.b).

The figures containing the vertical and horizontal components of displacement for the surface receivers in Model II are found in Figures (12) and (13). The PP reflection coefficient related to the halfspace/Wedge I interface is shown in Figure (6.b) and the surface conversion coefficients are the same as for Model I. Again, as in the Model I surface recorded synthetics there are three panels in Figures (12) and (13).

Only the total traces (reflected + diffracted) are shown for Model III in Figures (14.a) and (14.b). The vertical and horizontal components are the arithmetic sum of the corresponding traces for Model I and Model II.

CONCLUSIONS

A few simple geological models have been considered in which some of the basic concepts of diffraction theory in elastic media were presented. This was done within the framework of asymptotic ray theory (ART) and certain extensions thereof. ART produces results equivalent to those derived using the high frequency geometrical optics solution method. The models were designed to investigate properties of edge diffraction from a 3D wedge. Specifically, the introduction of the boundary ray for different geometries and ray types were considered. This ray is such that it defines the illuminated and shadow zones for reflected and direct arrivals. The diffracted exist in both regions while the direct/reflected only exists in the illuminated region. The formulae for the edge diffracted arrival were obtained from other works cited here. The smooth transition of the diffracted arrival across the boundary ray from one region to another was taken as an indication that the formulae being used satisfied at least that constraint. Comparison of the modified ART solution for this problem has been checked by others for more complex media and as such was not included here. The diffraction coefficient is a function of the difference of the diffracted and direct/reflected travel times. As the direct/reflected arrival does not exist in the shadow zone it was necessary to introduce the concept of analytic continuation to provide an appropriate value for this quantity. This report is not a definitive source of all theory that is required for the introduction of edge diffracted arrivals into synthetic traces for complex structures, but rather a simple introduction to the topic.

REFERENCES

Abramowitz, M. and Stegun, I.A. 1980, Handbook of mathematical functions, U.S. Government Printing Office, Washington.

Červený, V. and Ravindra, R. 1970, Theory of seismic head waves, University of Toronto Press, Toronto.

Červený, V. and Hron, F., 1980, The ray series method and dynamic ray tracing for three dimensional inhomogeneous media, Bull. Seism. Soc. Am., **70**, 47-77.

Červený, V., 2001, Seismic Ray Theory, Cambridge University Press, Cambridge.

Chan, G.H., 1986, Seismic diffraction from wedges, Ph.D. Thesis, University of Alberta, Edmonton.

Daley, P.F., 1990, Unpublished notes on diffraction theory for seismic applications.

Hron, F., 1986, Unpublished notes on diffraction theory for seismic applications.

Hron, F. and Kanasewich, E.R., 1971, Synthetic seismograms for deep seismic sounding studies, Bulletin of the Seismological Society of America, **61**, 1169-1200.

Gautschi,W., 1969, Complex error function, Comm. ACM, **12**, 363.

Gautschi,W., 1980, Error function and Fresnel integrals, Chapter 7 in: Handbook of Mathematical Functions, M. Abramowitz and I.A. Stegun, Editors., U.S. Government Printing Office, Washington.

Gel'chinsky, B.Y, 1961, Expression for the spreading function, Problems in the Dynamic Theory of Seismic Wave Propagation, **5**, (in Russian).

Klem-Musatov, K.D., 1980, Theory of edge waves and their use in seismology, NAUKA (in Russian).

Klem-Musatov, K.D., 1995, Theory of edge waves and their use in seismology, SEG Publications, F. Hron and L.R. Lines, Editors.

Klem-Musatov, K.D., Aizenberg, A.M., Pajchel, J. and Helle, H.B., 2007, Edge and tip diffractions: theory and applications in seismic prospecting, SEG Publications, P.F. Daley and L.R. Lines, Editors.

Mikhailenko, B.G., 1985, Numerical experiment in seismic investigation, Journal of Geophysics, **58**, 101-124.

Mikhailenko, B.G., 1988, Seismic fields in complex media, Academy of Sciences of the U.S.S. R., Siberian Division, (in Russian).

	P Velocity (km/s)	S Velocity (km/s)	Density (gm/cm^3)
Wedge I	**2.50**	**1.44**	**2.20**
Halfspace	**2.00**	**1.15**	**1.80**

Table 1. Geological parameters for Model I.

	P Velocity (km/s)	S Velocity (km/s)	Density (gm/cm^3)
Wedge II	**1.60**	**0.92**	**1.50**
Halfspace	**2.00**	**1.15**	**1.80**

Table 2. Geological parameters for Model II.

APPENDIX A

Assume a point source of compressional (P) waves located at the origin of an isotropic 3 dimensional Cartesian half space in which there is embedded a wedge of infinite dimensions in the y direction. At a time after an impulsive excitation of the point source the direct wavefront will have progressed to the define the wavefront surface at τ_G. Wavefronts resulting from reflection from the top of the wedge and transmission through it have not been considered. However, the diffracted wavefront from the impinging of the wavefront originating at the origin on point $\mathcal{D}$ is included. This diffracted wavefront defined by τ_D will be assumed to be propagating in the halfspace. The ray associated with the point source at the origin which is such that it passes some small distance $\varepsilon : \varepsilon \to 0$ front the point $\mathcal{D}$ and denoted R_B will be called the boundary ray. This ray separates the illuminated zone (Ω_I) from the shadow (Ω_S) zone for the direct wavefront which originates from a point source at some arbitrary origin, O.

In the shadow zone the direct geometrical arrival does not exist even though its travel time in this region is required to determine the argument of the diffraction coefficient, $\mathrm{W}(\mathrm{z})$, where

$$\mathrm{z} = e^{i\pi/4}\sqrt{\omega/2}\, w \tag{A.1}$$

and w is defined through the relationship

$$w^2 = \left[\frac{2\omega}{\pi}\left(\tau_{\mathcal{D}}(M) - \tau_G(M)\right)\right]. \tag{A.2}$$

In the shadow region the travel time of this arrival to the point M must be determined by analytic continuation of $\tau_G(M_0)$ from the shadow/illuminated boundary into the shadow region. As S_T is the tangent plane to $\tau_G(M_0)$ on the boundary ray R_B it may be interpreted as the local representation of $\tau_G(M_0)$ there, which is to say that from the view point of seismic energy partitioning due to encounters of the ray with interfaces it is identical to a seismic plane wave at that point. From a mathematical point of view the analytic continuation of the travel time along the plane representation of the wave front S_T requires that the travel time is the same along the plane wave front as it is at M_0. The same argument may be used to infer that the amplitude along the plane wave front S_T must also be the same as its value at M_0.

Using the coordinate system (ρ, ψ) defined in the text which is centered at the diffraction point $\mathcal{D}$, assuming that all rays are constrained to lie in the (x, z) plane of the (x, y, z) Cartesian system initially assumed here, the travel time of the direct geometrical arrival on the seismic boundary ray R_B, is $\tau_G(M_0)$ and as a result of the preceding argument

$$\tau_G(M) = \tau_G(M_0) \quad \text{where} \quad M \in S_T . \tag{A.3}$$

If τ_1 is the time taken for the direct geometrical arrival to travel from the point source to the diffraction point $\mathcal{D}$, then

$$\tau_D(M) = \tau_1 + \rho_M / \alpha \tag{A.4}$$

and

$$\tau_G(M) = \tau_1 + \rho_M \cos\psi_M / \alpha \tag{A.5}$$

where α was defined in the text as the P wave velocity in the half space. Substituting equations (A.4) and (A.5) into (A.2) the quantity z expressed in terms of w may be obtained from

$$w^2 = \left[\frac{2\omega}{\pi}\left(\tau_{\mathcal{D}}(M) - \tau_G(M)\right)\right] = \left[\left(\frac{2\omega}{\pi}\right)\left(\frac{\rho_M}{\alpha}\right)\left(1-\cos\psi_M\right)\right]. \tag{A.6}$$

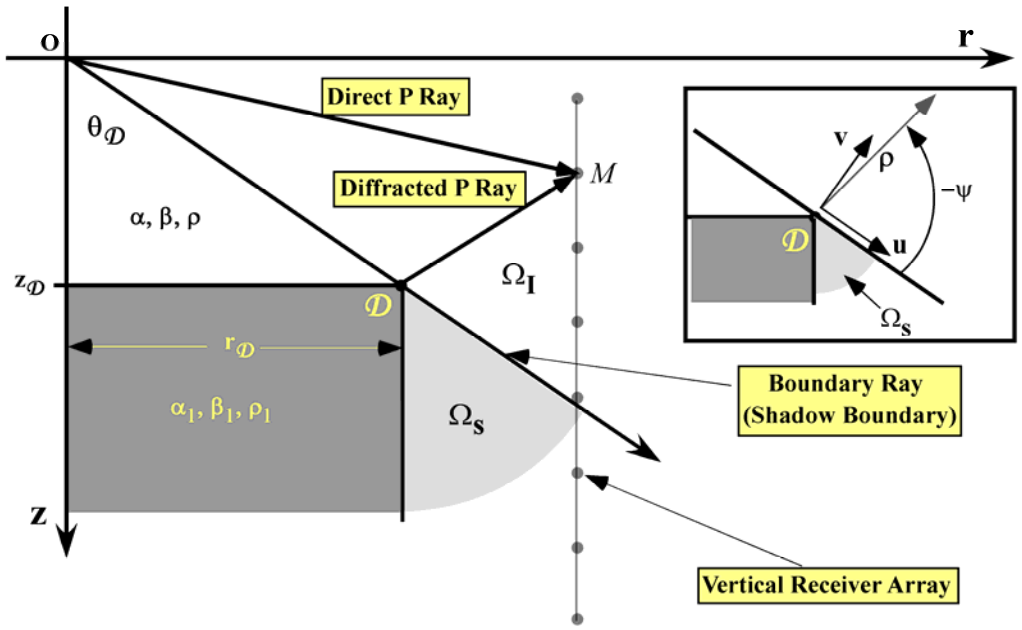

FIG. 1. Geometry of Model I for a vertical array of receivers.

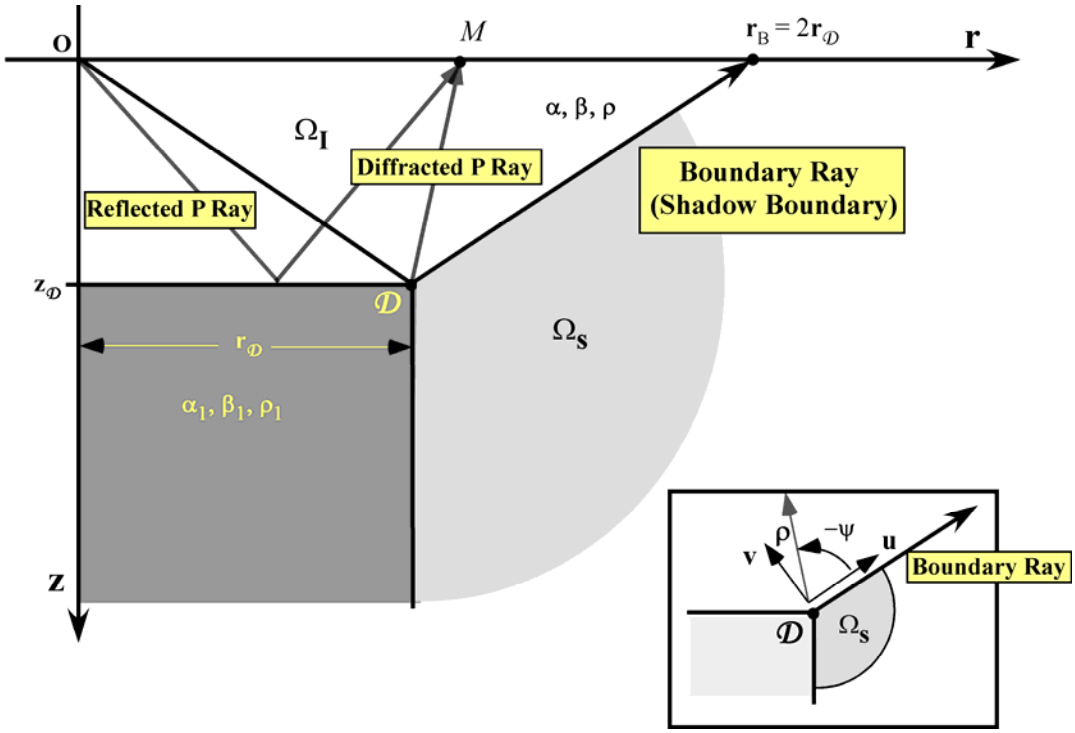

FIG. 2.. Geometry of Model I for an array of receivers located at the surface.

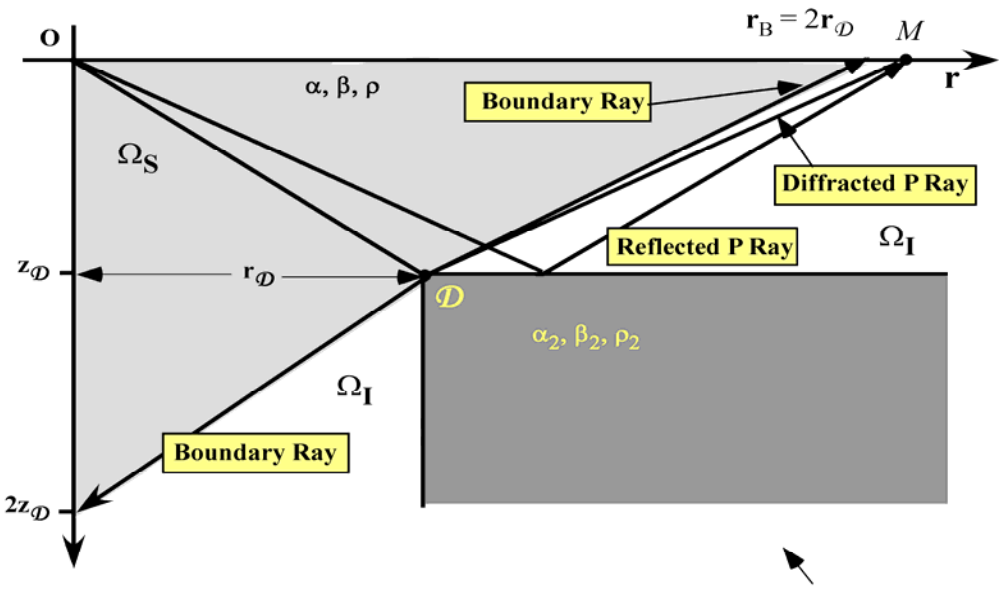

FIG 3.. Geometry of Model II for an array of receivers located at the surface. Also shown, but not used here, is the boundary ray for reflections from the flank of the wedge and the corresponding shadow and illuminated zones.

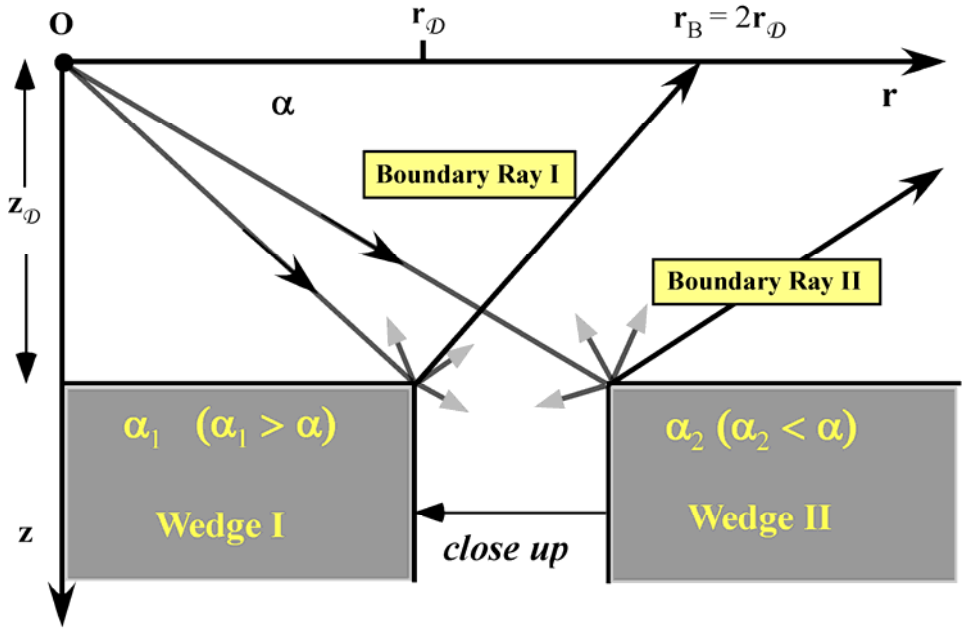

FIG. 4.. Geometry for Model III.

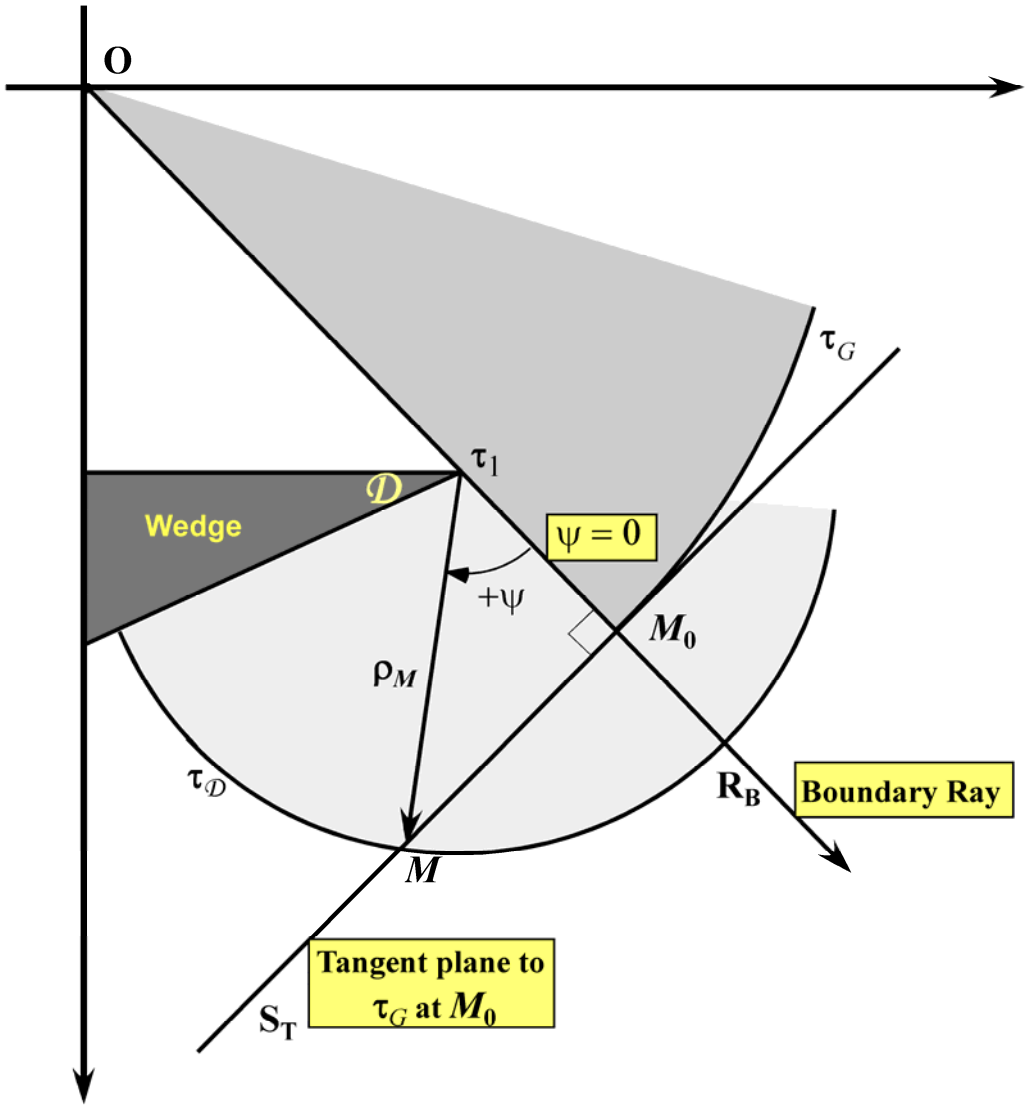

FIG. 5. Analytic continuation of the spherical geometrical wavefield into the shadow region. See Appendix A for a more complete discussion.

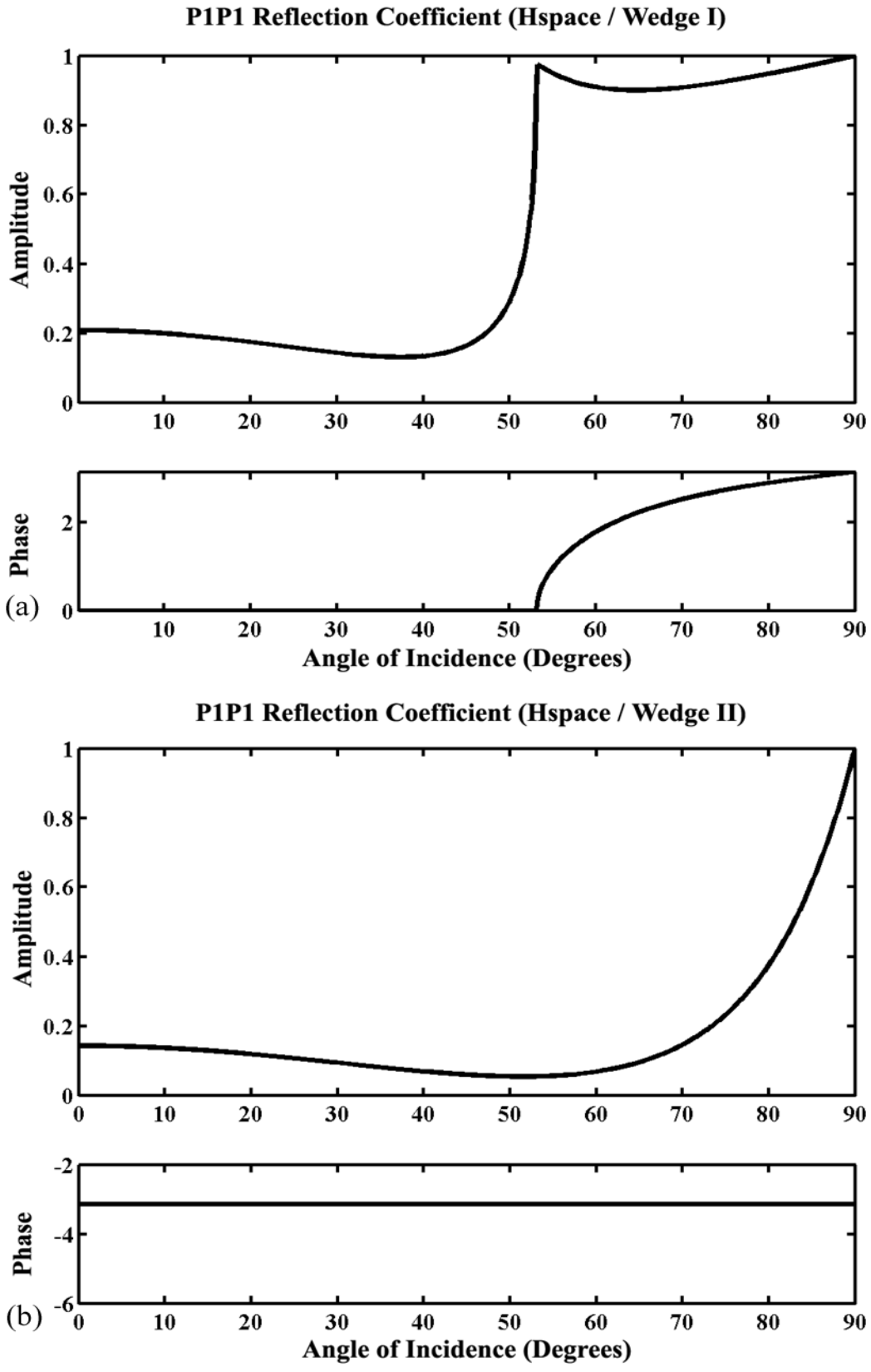

FIG. 6. *PP* reflection coefficients for Models I (a) and II (b). See Tables I and II for more details.

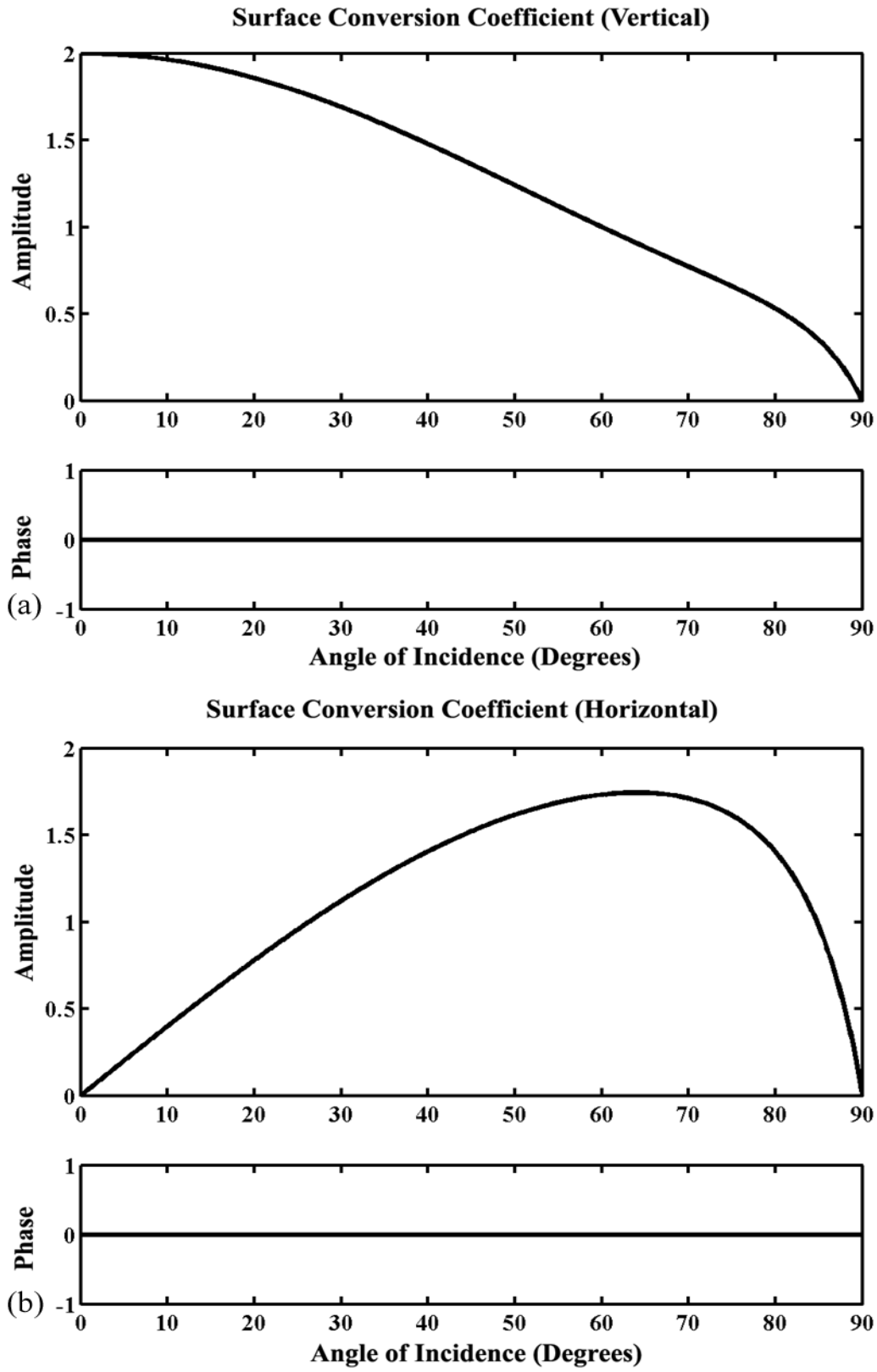

FIG. 7. Vertical (a) and horizontal (b) components of the surface conversion coefficient vector for Models I, II and III, used for both reflected and diffracted waves at surface receivers.

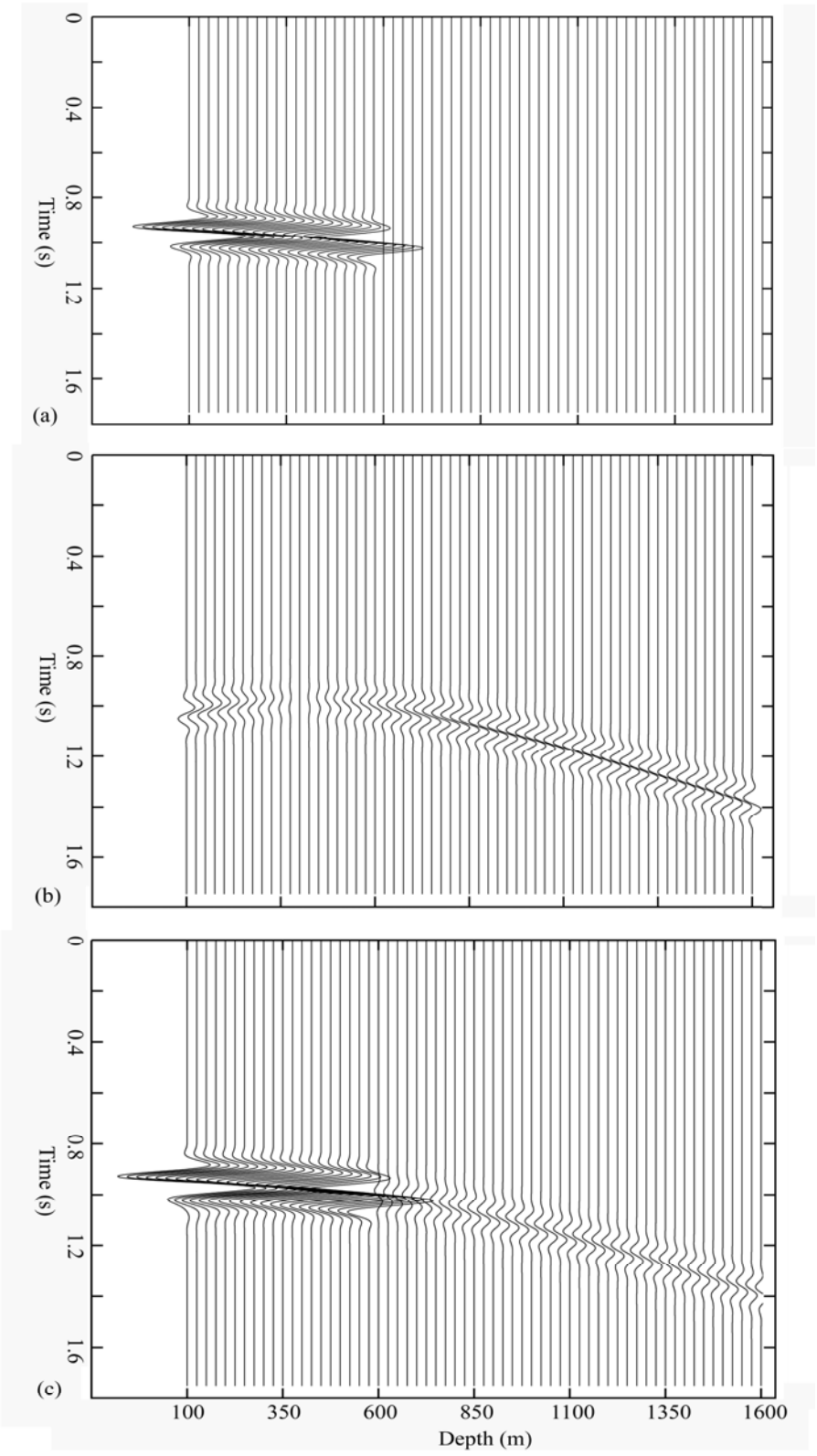

FIG. 8. Vertical component of displacements of the (a). direct, (b). diffracted and (c). combined, PP_r^V , for Model I (VSP).

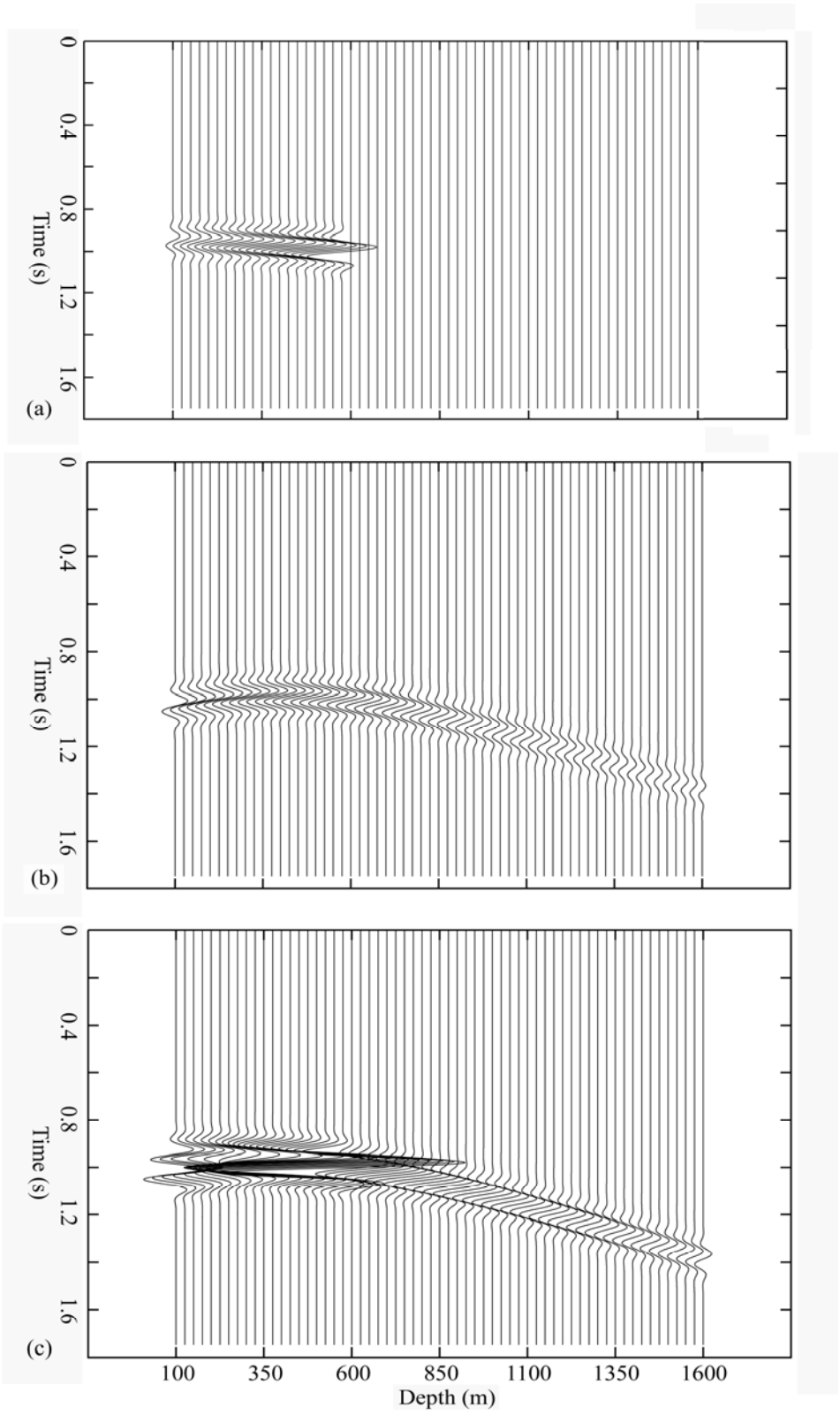

FIG. 9. Horizontal component of displacements of the (a). direct, (b). diffracted and (c). combined, PP_r^H , for Model I (VSP).

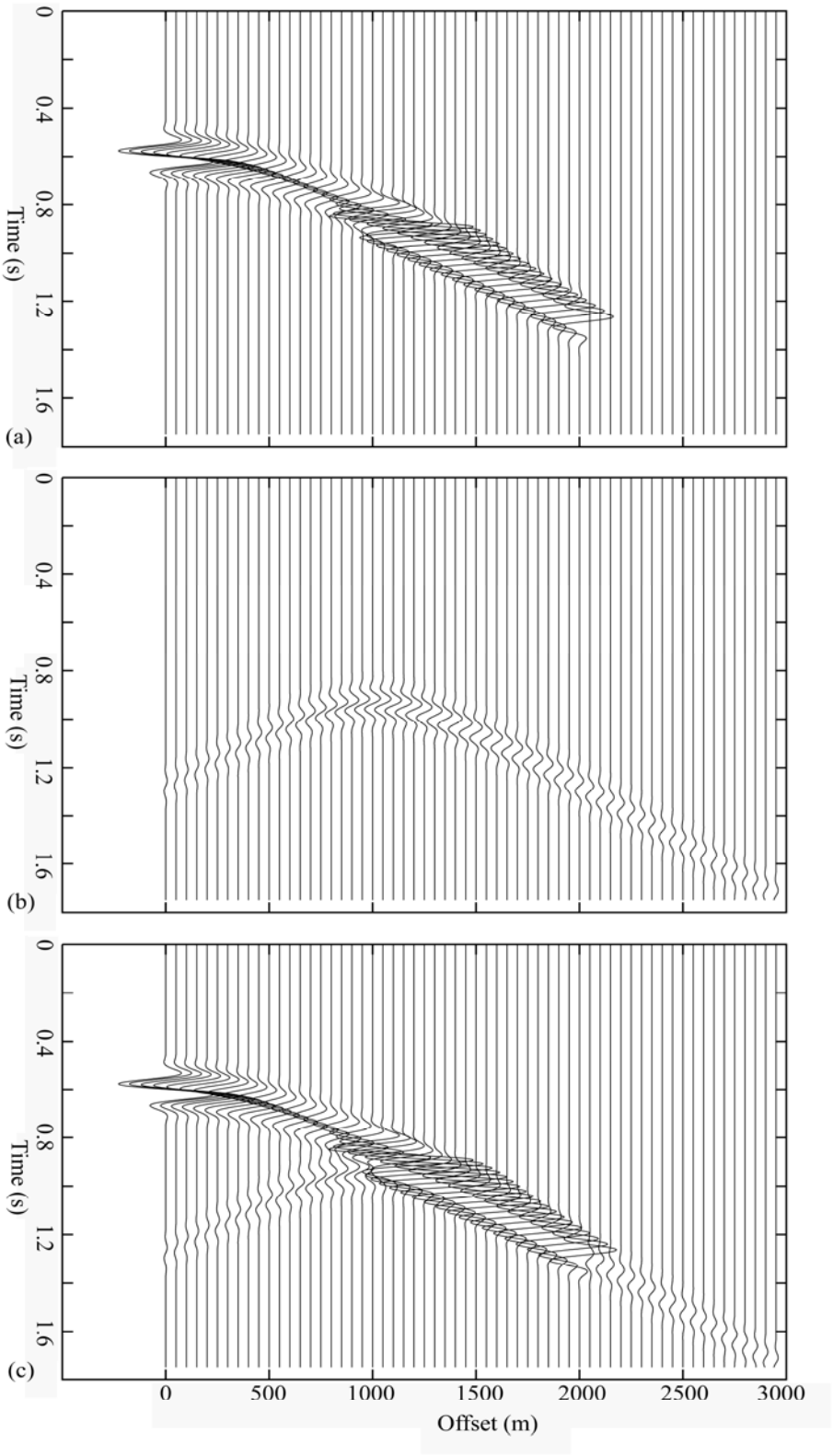

FIG. 10. Vertical component of displacements of the (a). reflected, (b). diffracted and (c). combined, PP_r^V , for Model I (Surface receivers).

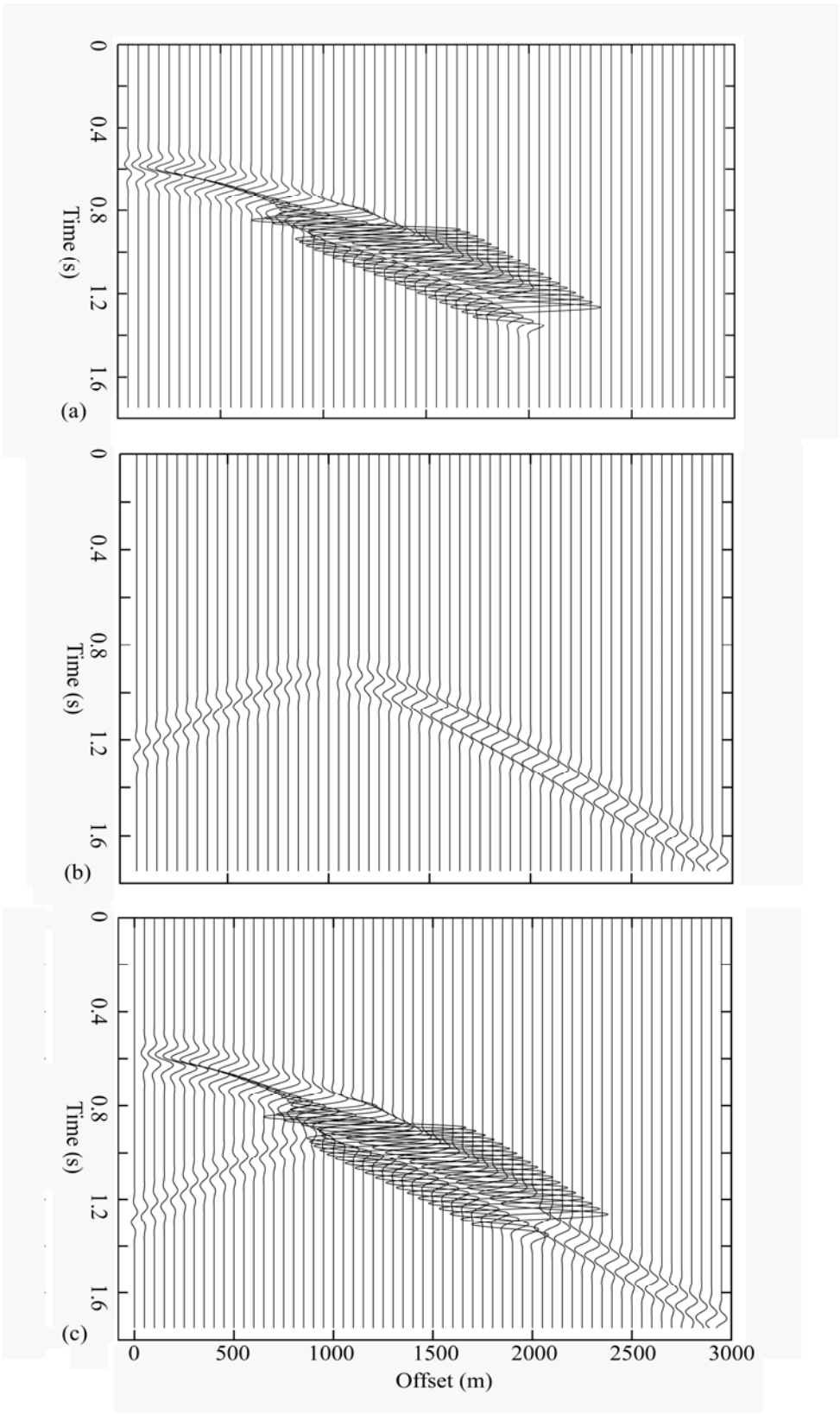

FIG. 11. Horizontal component of displacements of the (a). reflected, (b). diffracted and (c). combined, PP_r^H , for Model I (Surface receivers).

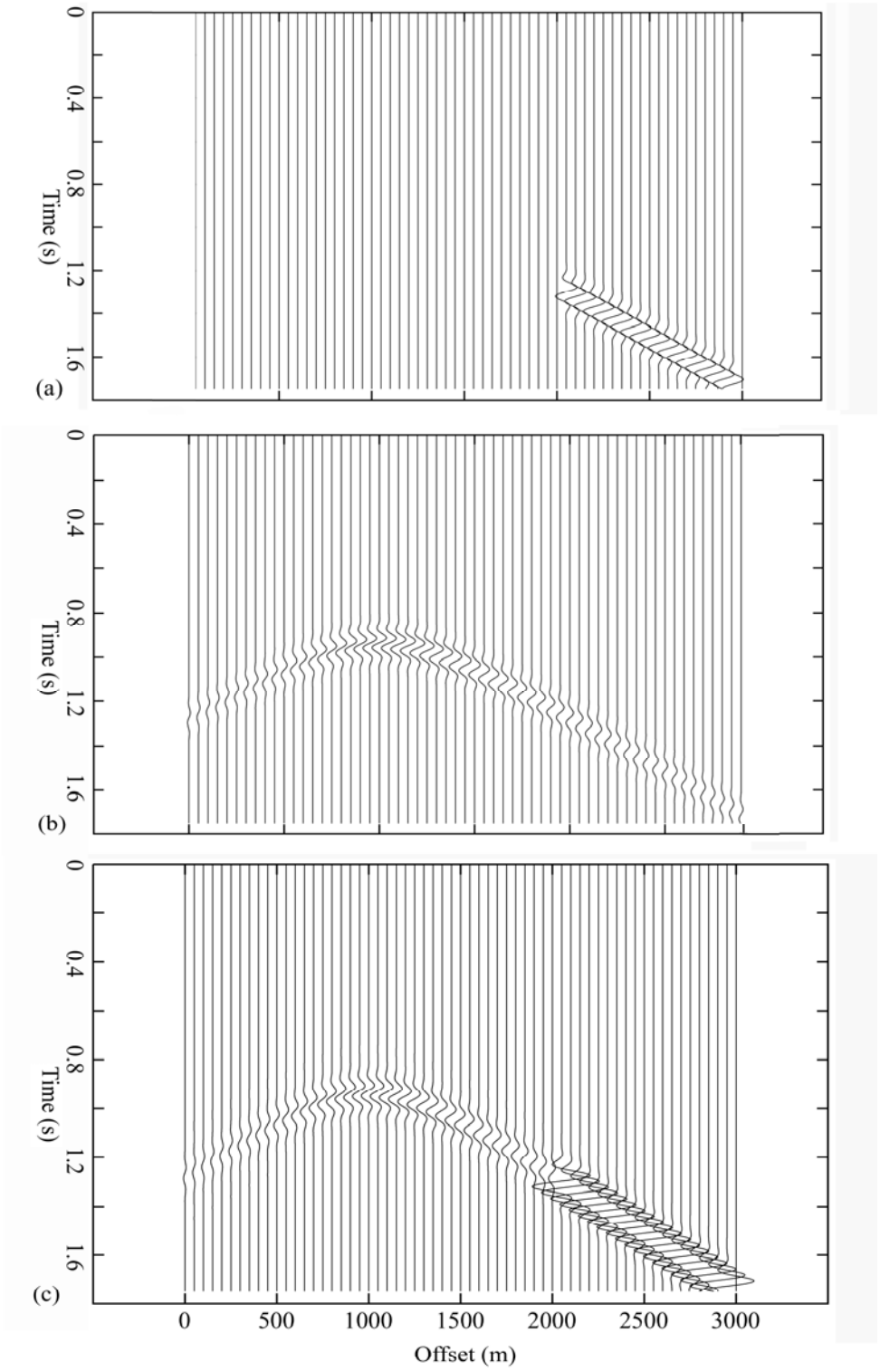

FIG. 12. Vertical component of displacements of the (a). reflected, (b) diffracted and (c) combined, PP_r^V , for Model II (Surface receivers).

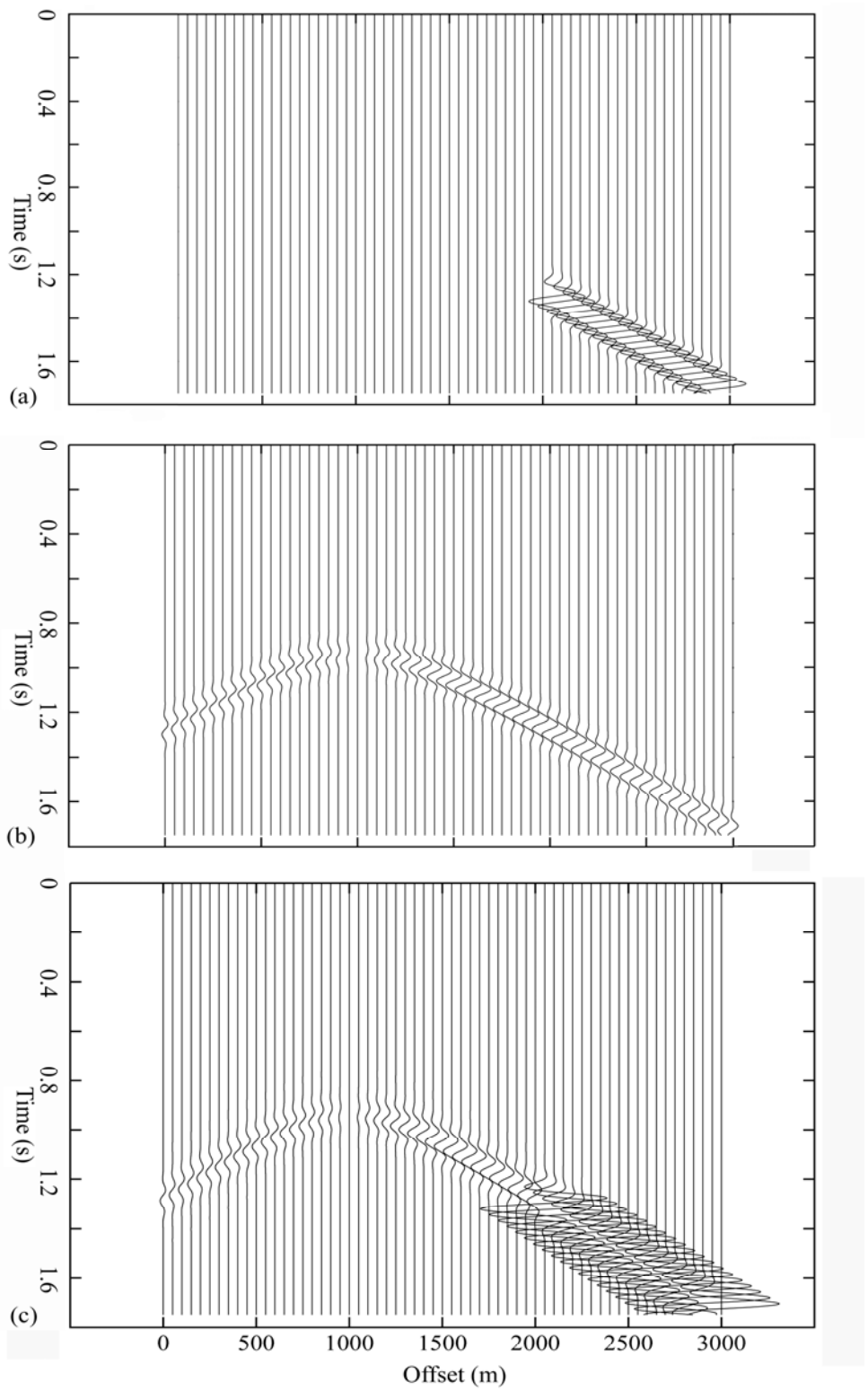

FIG. 13. Horizontal component of displacements of the (a). reflected, (b) diffracted and (c) combined, PP_r^H , for Model II (Surface receivers).

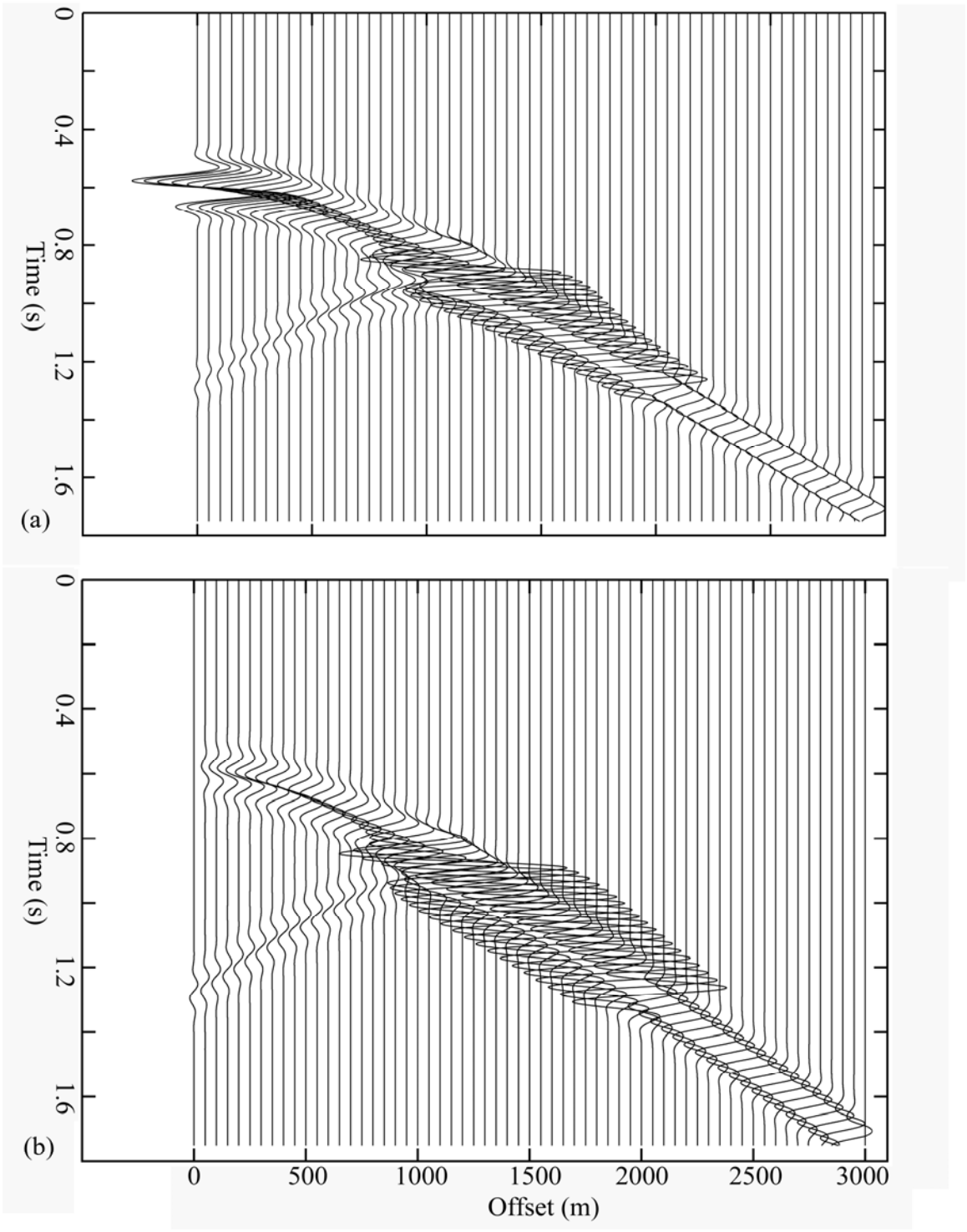

FIG. 14. Vertical (a) and horizontal (b) components of displacement of the combined, PP_r^V and PP_r^H for Model III (Surface receivers).